https://doi.org/10.33271/nvngu/2025-5/069

Ya. Frolov[1],
orcid.org/0000-0001-6910-6223,
F. Nuernberger[2],
orcid.org/0000-0002-7824-0675,
D. Konovodov[*1],
orcid.org/0000-0001-8282-4991,
O. Bobukh[1],
orcid.org/0000-0001-7254-3854,
V. Boiarkin[1],
orcid.org/0009-0005-7582-9504

1 – Ukrainian State University of Science and Technology, Dnipro, Ukraine
2 – Leibniz Universität Hannover, Hannover, Federal Republic of Germany
[*] Corresponding author e-mail: d.v.konovodov@ust.edu.ua

INFLUENCE OF DEFORMATION PARAMETERS ON MECHANICAL BEHAVIOUR OF ALUMINIUM-MAGNESIUM ROLL-BONDED COMPOSITES WITH KIRIGAMI-STRUCTURED INLAYS

Purpose. To assess how the mechanical properties of a composite material comprising EN AW 1050 aluminium, and kirigami-inspired structure made from E235 steel and AZ31 magnesium alloy, depend on the initial configuration of its components and the degree of reduction during roll bonding.

Methodology. The study involved roll-bonding five-layer composite sheets with the following configuration: two of the internal layers consisted of a kirigami structure implemented using an expanded metal mesh made from low-carbon steel. The outer matrix layers were aluminium alloy sheets, and the core matrix layer was formed from magnesium alloy sheets. The transformation of the kirigami structure within the composite was assessed using X-ray analysis. The mechanical properties of the composites were evaluated using three methods: impact bending tests, three-point bending tests and ball indentation tests.

Findings. Experimental investigations yielded data on how the kirigami structure transforms within the five-layer composite, depending on the rolling reduction. It was found that a rolling reduction of 55 % provided an isotropic mechanical response. Mechanical testing showed that the energy absorption capacity was enhanced by 60–70 % with kirigami inlay, even under complex stress–strain conditions. The stiffness of the reinforced composite was found to be several times higher than that of unreinforced aluminium.

Originality. This study is the pioneer in analysing the combined effect of component configuration and rolling reduction on the mechanical behaviour of a five-layer aluminium-magnesium composite reinforced with a steel kirigami structure. The study demonstrated that deformation parameters ensured reliable bonding between the aluminium and magnesium layers and significantly enhanced mechanical performance by controlling the transformation of the kirigami structure.

Practical value. The findings of this study enhance our understanding of how rolling reduction and initial layer configuration affect the deformation behaviour of multilayer Al-Mg composites. They also lay the groundwork for designing novel composites reinforced with kirigami structures for advanced structural applications.

Keywords: *roll bonding, kirigami structure, composite material, specific strength*

Introduction. An important area of development for thermomechanical treatment technologies is to increase the mechanical properties of structural materials, particularly stiffness and impact energy absorption. One approach in this area is the development of hybrid composite materials made of magnesium and aluminium. Combining these metals in multilayer Al/Mg/Al composites creates a synergistic effect, providing balanced performance characteristics. Among the current techniques of manufacturing metal composites, roll bonding technology is distinguished for its adaptability and productivity, merging the benefits of pressure welding and severe plastic deformation.

A pioneering way to the problem of enhancing the performance of composites is the utilisation of steel cut-and-pull mesh inlay, inspired by the principles of kirigami. Such an innovative technique involves the formation of a geometrically modified shape during the roll bonding process between aluminium and magnesium layers. This allows for the introduction of mechanisms to enhance the material's strength, as well as improving the bond between the layers. The plastic flow of the aluminium and magnesium matrix activates the inhomogeneous deformation of the kirigami structure. This, in turn, restricts the flow, resulting in a complex stress-strain state in the deformation zone, particularly within the magnesium layer, thereby increasing its deformability.

This study aims to assess the impact of component configuration and deformation parameters on the mechanical properties of a five-layer, three-component composite consisting of an aluminium alloy (EN AW 1050), a magnesium alloy (AZ31) and a steel kirigami inlay.

Literature review. An effective way of improving mechanical properties such as strength, ductility, stiffness, impact resistance and wear resistance is to use hybrid composite materials made from different metals [1]. Due to their advantages, magnesium and aluminium alloys are widely used in transport and other engineering fields as lightweight structural materials [2]. Magnesium alloys have the lowest specific gravity of all structural metals. They are characterised by their high specific strength and stiffness, as well as their excellent damping properties [3]. At the same time, aluminium and its alloys offer excellent corrosion resistance in acidic environments and can be easily deformed [4]. Thus, Al-Mg-Al composites offer a combination of the advantages of each component, expanding the range of applications.

Roll bonding is the most appropriate method for industrial use among the various methods for producing composites due to its stability, simplicity, efficiency and easy mass production. The process of hot roll bonding, which is conducted at temperatures that exceed the recrystallisation temperature, facilitates plastic deformation and dynamic diffusion exchange of atoms between dissimilar materials. Nevertheless, there are certain challenges associated with the integrity of the bond [5, 6]. Increasing the rolling temperature to 400 °C enhances the joint's strength by improving diffusion between the aluminium and magnesium layers [7]. Rolling with a 20 % reduction at temperatures above 400 °C allows for a strong bond between workpieces made of 1,060 aluminium alloy and AZ31 magnesium alloy. Study [8] have also shown that increasing the rolling temperature from 400 to 420 °C promotes grain growth and excessive growth of the diffusion layer, reducing the strength of the joint. The optimum rolling temperature varies depending on the alloy, since aluminium and magnesium alloys exhibit different deformation behaviour and microstructure changes under rolling conditions.

Preventing surface oxidation is critical to achieving a high-quality joint. Excessively high rolling temperatures promote oxidation, resulting in poor diffusion and metal sticking to the rolls [9]. Methods such as hot roll bonding and two-pass rolling are used to reduce oxidation. In the latter case, the initial joint is formed at 350 °C in the first rolling step, and the second rolling step is performed at 400 °C to increase compression and enhance diffusion. Pre-joining methods such as hot pressing, extrusion or welding can also be implemented to minimise oxidation during high-temperature roll bonding [10].

Rolling reduction is important for achieving a metallurgical bond between the layers. Insufficient reduction fails to break down the oxide layers, thereby limiting metal-to-metal contact. Ideally, reduction should break the oxide layers, improve metal-to-metal contact and promote grain refinement. However, excessive deformation can cause defects and reduce the quality of the bond. However, excessive compression can lead to significant edge cracking, which has a negative impact on the composite's performance [11, 12]. For multilayer magnesium/aluminium metal composites, the reduction value is typically between 20 and 80 %. The maximum reduction value during roll bonding depends on the deformability of the alloys. For example, for the AZ31 – EN-AW 1060 pair, it is 20 %. Moderate reduction (20–50 %) creates a fine-grained, homogeneous structure that increases strength and ductility [13]. However, excessive reduction (60–80 %) at high temperatures (400 °C) can reduce joint strength due to grain enlargement and diffusion layer thickening [14, 15]. Consequently, the rolling reduction value should be optimised by considering the material's ductility, microstructure evolution and bond strength between phases [16].

A new trend in the production of flat, roll bonded composites involves using a steel, expanded mesh inlay – a technique inspired by kirigami. Kirigami, an ancient art of cutting sheets of material, has recently gained popularity due to advances in computer modelling and its application in various fields, including energy conservation, flexible electronics, and structural mechanics [17]. The potential for deformation of kirigami structures extends beyond the limits of their base materials. This is achieved by introducing controlled cutouts that create zones of high and low stress. In these zones, localised bending deformations are promoted instead of homogenous tension [18].

Recent studies have confirmed the effectiveness of kirigami inserts in roll bonding mesh-structured composites. For instance, roll bonding of mesh structures has successfully been applied to AISI 304 stainless steel and AISI 1010 mild steel, thereby improving their mechanical performance. By optimising the shape and size of the cuts, researchers have increased tensile strength, with curved cuts yielding slightly better results than straight ones [19]. The effect of uneven stress during rolling has been well studied in relation to thin-walled tubes and biomedical stents.

In the context of roll bonding aluminium alloy EN AW 1050 as the matrix and magnesium alloy AZ31 as the inlay [20], introducing steel expanded mesh for reinforcement could further enhance the composite's mechanical properties. The behaviour of the kirigami structure in rolled composites is determined by the dynamic equilibrium of the mechanical and ductile properties of the inlay and matrix during common deformation. A soft matrix, such as the aluminium alloy EN AW 1050, promotes greater axial flow in the deformation zone. This increases the opening angle of the kirigami structure and narrows its lines [21, 22]. Conversely, the hard matrix restricts the bending of the lines, resulting in the kirigami structure flattening rather than stretching. These deformation characteristics are key to the mechanical properties of the roll-bonded composite, making mesh reinforcement a valuable strategy for improving the structural performance of Mg-Al composites [23].

Using the kirigami structure during the roll bonding process for Mg-Al hybrid composites unlocks the potential of each material component by enabling directed, localised deformation in the cut zones. The uneven stress distribution caused by the kirigami inlay's complex geometry contributes to the multiplication of the mechanical effect, activating additional strengthening mechanisms and increasing deformation intensity. This approach improves not only the bonding between the layers, but also enhances the composite's properties synergistically, opening new opportunities for its use in innovative engineering.

Purpose. This study aims to assess how the mechanical properties of a composite material comprising EN AW 1050 aluminium, and kirigami-inspired structure made from E235 steel and AZ31 magnesium alloy, depend on the initial configuration of its components and the degree of reduction during roll bonding.

Methodology of experimental research. ***Roll bonding.*** Fig. 1 shows the general scheme for roll bonding a five-layer, three-material composite with a double kirigami inlay.

The scheme shown in Fig. 1 illustrates the process of common rolling a symmetrical five-layer assembly consisting of individual layers, as shown below (example)

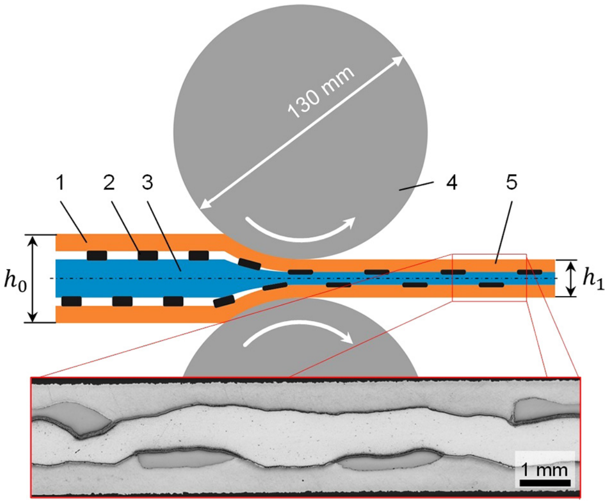

Fig. 1. Scheme of roll bonding of five-layer, three-material composite sheets reinforced with two kirigami structures:

h_0 – initial assembly thickness; h_1 – final sheet thickness; 1 – outer matrix sheet (EN AW 1050); 2 – flat kirigami structure (E235 steel); 3 – inner matrix sheet (AZ31); 4 – rolls with a diameter of 130 mm; 5 – composite sheet

$$\mathrm{Al}_i + Ki_{0.5} + AZ31_j + Ki_{0.5} + \mathrm{Al}_i,$$

where Al_i is an aluminium sheet EN AW 1050, whose thickness varied during the experiments; $Ki_{0.5}$ is a sheet of kirigami structure made from 0.5 mm-thick E235 steel expanded mesh; $AZ31_j$ is a sheet of $AZ31$ magnesium alloy, whose thickness also varied during the experiments.

The rolling reduction during roll bonding is calculated as follows

$$\varepsilon_{hi} = \frac{h_0 - h_i}{h_0} \cdot 100\ \%\ , \tag{1}$$

where h_0 is the sum of the assembly components thicknesses; h_i is the thickness of the rolled composite after the i^{th} pass.

The composites were roll bonded when the shape factor, defined as the ratio of the length of the deformation zone to the average thickness of the sheet, was between 2.9 and 4.0.

The following heat treatment was applied to bring the materials to a ductile state:

1. EN AW 1050 – exposure at 550 °C for 10 minutes, then free air cooling.
2. AZ31 – exposure at 400 °C for 10 minutes, then free air cooling.
3. E235 – 720 °C for 5 minutes, then free air cooling.

Table 1 shows the mechanical properties of the components' materials based on the results of tensile tests, as well as their density values.

The components of the assembly were cut into 70 × 100 mm pieces and fastened with rivets.

The kirigami structure in this study was made using a rhombic expanded mesh. The material used was low-carbon steel E235, with a sheet thickness of $t = 0.5$ mm. The dimensions of the mesh cell are shown in Fig. 2.

Inserting a steel kirigami structure between the aluminium and magnesium matrix increases the specific weight or density of the composite. This value ρ_C, obtained by dividing the measured weight of the composite m_C, by its measured volume V_C, should lie between the densities of the aluminium matrix ρ_{Al}, and the steel kirigami structure ρ_{Ki}. Comparing ρ_C with ρ_{Al} reveals the weight characteristics of the composite. It is convenient to evaluate this in terms of the density increase factor

Table 1

Tensile properties and density of the materials used in the components

Material	Yield stress, MPa	Ultimate tensile stress, MPa	Density, g/cm^3
AZ31	200	260	1.8
EN AW 1050	20	75	2.9
E235	240	350	7.8

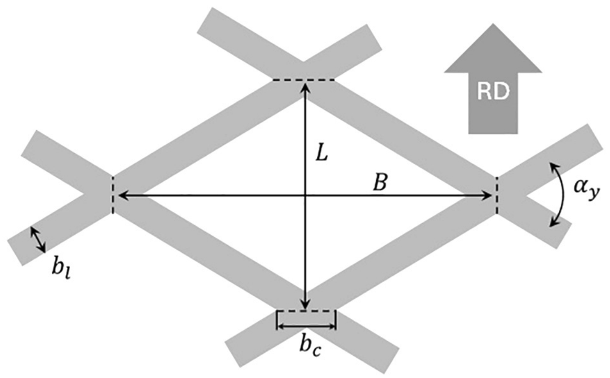

Fig. 2. Mesh cell dimensions:

L = 6 mm – cell length; b_1 = 3.7 mm – cell width; b_c = 0.5 mm – knuckle width; α_y = 62° – longitudinal mesh angle; RD – rolling direction

$$DI = \rho_{Al} + \frac{\rho_c - \rho_{Al}}{\rho_{Al}}. \tag{2}$$

This study focuses on three types of composites shown in Table 2. These composites were produced using a duo mill with 130 mm diameter rolls at a temperature of 400 °C and a rolling speed of 0.29 m/s.

Before rolling, the surface of all composite components was degreased and cleaned with an abrasive. The composites underwent a final softening heat treatment at a similar temperature for 10 minutes.

A series of tests were performed at room temperature to evaluate how the initial thickness of the assembly layers and the roll bonding mode affect the mechanical properties of the composites.

Impact bending test. Impact bending tests were carried out using a pendulum impactor with an impact energy of 15 J and a gap of 30 mm. The dimensions of the samples were: $h_i \times b \times 50$ mm, where h_i is the thickness of the composite after rolling and b is the width of the specimen. The width of the specimens was 17 mm. This value was chosen so that the width of the specimen would contain as many mesh cross-sections as possible for representative results. However, this was limited by the design of the testing machine. There were no cuts or other artificial defects on the specimen's surface.

Three-point bending. The three-point bending test was performed in accordance with ISO 178 with the following parameters: specimen length l = 130 mm; width

Table 2

List of experiments with assembly configuration and rolling parameters

Experiment code	Assembly configuration	Roll. pass	h_0, mm	h_i, mm	ε_{hi}, %	ε_{Σ}, %	*DI* (2)
C1	$Al_{1.5} + Ki_{0.5} + AZ31_{1.8} + Ki_{0.5} + Al_{1.5}$	1	5.80	3.20	45	70	1.03
		2	3.20	1.73	46		
C2	$Al_{1.0} + Ki_{0.5} + AZ31_{1.8} + Ki_{0.5} + Al_{1.0}$	1	4.80	3.15	34	64	1.04
		2	3.15	1.73	45		
C3	$Al_{1.0} + Ki_{0.5} + AZ31_{1.5} + Ki_{0.5} + Al_{1.0}$	1	4.50	2.20	51	51	1.11

b = 20 mm; thickness h_i varied for each composite; bending edge radius R_1 = 10 mm; support radius R_2 = 10 mm; span length L = 60 mm. Movement of the bending supports was stopped when the deflection D = 30 mm. The test speed was 1,000 mm/min. The test resulted in a load-deflection curve, which was used to determine the following parameters:

1. Flexural stress, MPa

$$\sigma_f = \frac{3FL}{2bh_i^2}.$$

2. Flexural strain

$$\varepsilon_f = \frac{6Dh_i}{L^2} \cdot 100\ \%.$$

3. Tangent modulus of elasticity

$$E_f = \frac{L^3 m}{4bLh_i^2},$$

where m is the slope of the tangent to the initial straight section of the load-bending curve (N/mm).

4. Flexural yield stress $\sigma_{0.2f}$.
5. Maximal flexural stress $\sigma_{\max f}$.

Ball indentation test. To evaluate the energy absorption ability of composites under bulk stress, we employed an original testing method involving indentation a hardened ball into the intersection point of the diagonals of a square specimen. The specimen is positioned on a tubular base so that the tube's axis passes through the point where its diagonals intersect. Tensile/compression tests are performed using a test machine, with load and displacement recorded. Specific force is the value obtained by dividing the load by the specimen's thickness. This value is used to compare the properties of specimens of different thicknesses.

Results of the study. The limiting factors in the experiments were:

1. Rolling force. The maximum rolling force that should be used for the rolling mill in the experiments is 200 kN. In experiment C3, the force reached 170 kN.

2. Mechanical bonding should occur during the first pass [24, 25]. The assembly's integrity is at risk of being compromised by delamination or even destruction if the layers do not bond adequately during the initial pass, due to the components' differing values of Young's modulus and coefficient of thermal expansion. For composite manufacturing to be successful, it is vital to ensure a reliable mechanical bond after the first pass.

3. Due to significant friction between the outer aluminium matrix and the rolls, and cooling of the outer assembly layers, the inner magnesium matrix experiences increased deformation. The kirigami structure tends to embed itself in the inner matrix, which is warmer and softer. This is why, the inner AZ31 alloy matrix was taken 20–80 % thicker than the single outer EN AW 1050 alloy matrix in our experiments.

4. A lack of control over the deformation of the kirigami structure can lead to excessive growth. In this case, the elements either collapse by themselves or destroy the internal matrix.

Roll bonding. Fig. 3 shows X-ray images of the kirigami structures that were deformed during the roll bonding inside the composite.

These images show that, in Experiment C1, the angle α_y increased to 118°, causing the kirigami structure to collapse at two points: the middle of the line and the intersection of the lines (knuckles). In experiment C2, in which the reduction was smaller than in C1 (Table 2), the angle α_y grew up to only 114°, and the structure broke at the knuckles. Experiment C3 achieved an angle α_y of 86°, which did not lead to the destruction of the kirigami structure. At the same time, the connection of the layers remained reliable.

This observation suggests that there is an equilibrium condition that ensures the continuity of the kirigami structure in the deformation zone, which is important for understanding the mechanics of this process. It can be formulated as follows: to preserve the kirigami structure during roll bonding, it is necessary that at any given time the total area of projections of all mesh lines onto the vertical transverse plane coincides with the total area of projections of the areas where these lines intersect each other.

The conditions for uniform deformation during the tensile stretching of a kirigami structure are also discussed in [21].

Assuming that the kirigami structure is uniformly thinned during the rolling process, this condition can be expressed as the ratio of linear dimensions

$$b_c \cos\frac{\alpha_y}{2} \approx 2b_l \sin\frac{\alpha_y}{2}, \quad (3)$$

where b_l is cell width; b_c is knuckle width; α_y is longitudinal mesh angle.

This approach does not consider the stress-strain state that occurs in composite components during roll bonding. Consequently, the area where the lines intersect undergoes complex deformation, including bending, stretching and flattening [13]. Nevertheless, condition (3) can be used effectively to select a rational kirigami cut shape.

Maintaining geometric consistency between the mesh elements is necessary to prevent the kirigami structure from being destroyed and the inner matrix from being damaged during rolling.

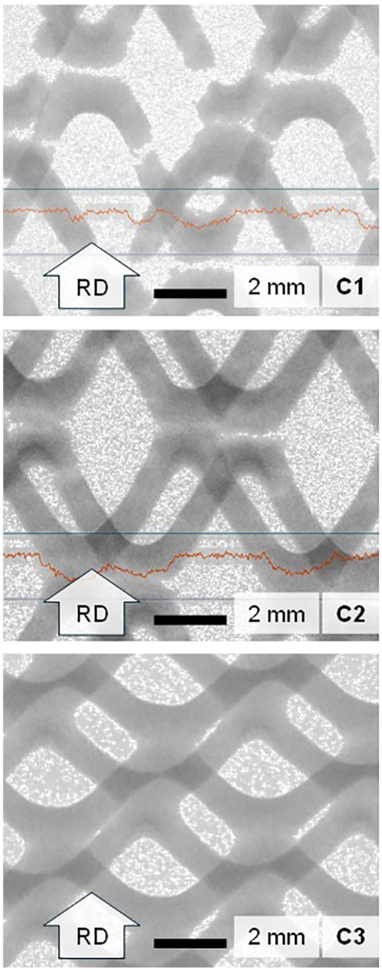

Fig. 3. X-ray images of kirigami structures inside rolled composite sheets after rolling and joining (Table 2):

$C_1 - \mathrm{Al}_{1.5} + Ki_{0.5} + AZ31_{1.8} + Ki_{0.5} + \mathrm{Al}_{1.5}$;
$C_2 - Ki_{0.5} + AZ31_{1.8} + Ki_{0.5} + \mathrm{Al}_{1.0}$;
$C_3 - \mathrm{Al}_{1.0} + Ki_{0.5} + AZ31_{1.5} + Ki_{0.5} + \mathrm{Al}_{1.0}$

Condition (3) is not satisfied for the mesh used as a kirigami structure in the experiments presented.

The value of the expression $2b_l \sin\frac{\alpha_y}{2}$, which describes the geometry of lines, was between 1.7 and 1.95 times greater than the value describing the geometry of the knuckle $b_c \cos\frac{\alpha_y}{2}$. This ratio restricted the degree of rolling reduction to 51 % in experiment C3.

Impact bending test. The energy absorbed by the specimens during the tests ranged from 1.6 J to 6 J.

The specimens (three for each point) did not fracture during the test. The test results can therefore be interpreted as showing the specific energy required to push a 50 mm-long specimen through a 30 mm-wide gap.

Since the thicknesses of the specimens tested are different, the specific impact energy value A'_{Imp} should be used to compare the energy absorbed by each one

$$A'_{Imp} = \frac{A_{Imp}}{h_i}, \qquad (4)$$

where A_{Imp} is energy absorbed by the specimen after impact, J; h_i is specimen thickness, mm.

Fig. 4 shows the results of impact tests on composites C1, C2 and C3 (Table 2), as well as on aluminium EN AW 1050 samples with a thickness of 2.2 mm.

A comparison of the impact bending test results showed that the C3 sample absorbed the highest impact energy, with the kirigami structure remaining intact after rolling. This was 66 % higher than the EN AW 1050 alloy sample. The kirigami structure in Sample C2 collapsed only where the lines intersected. This resulted in a 27 % higher value of A'_{Imp} being achieved. The presence of two fracture centres in the kirigami structure in experiment C1 (Fig. 3) reduced its ability to absorb impact energy compared to the aluminium sample.

Three-point bending. The results of the three-point bending tests of C1, C2 and C3 composites (Table 2) and 2.2 mm thick aluminium EN AW 1050 (Alu) are shown in Table 3.

The stress-strain curves for these samples are shown in Fig. 5.

As can be seen in Table 3, all composites demonstrated advantages in stiffness and higher flexural properties in the three-point bending tests compared to aluminium. The specimens after experiment C3 also exhibited enhanced deformability. They demonstrated increases by 7.8 times in elastic modulus, 2.8 times in yield strength, 2.7-fold in maximum flexural stress and 1.6 times in maximum flexural strain. Meanwhile, as shown in Table 2, the density of the composite increased by only 11 % compared to aluminium.

As shown in Fig. 5, the stress-strain curve and photographs of the specimens after three-point bending reveal differences in the behaviour of composites C1, C2 and C3. Specimen C1 exhibited the lowest strength in the test series, showing signs of brittleness and failing at a strain of 2.8 %.

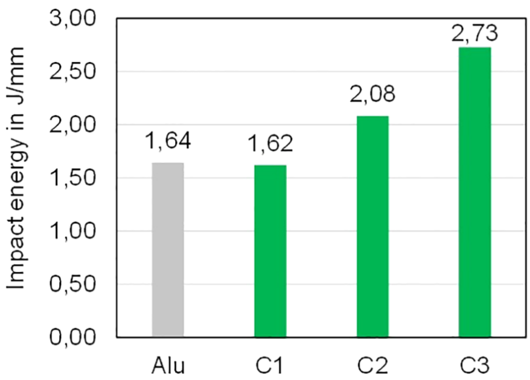

Fig. 4. Impact test results for aluminium alloy EN AW 1050 and rolled composites:

Alu – specimen of EN AW 1050; C1, C2 and C3 – roll bonded composites $\mathrm{Al}_i + Ki_{0.5} + AZ31_j + Ki_{0.5} + \mathrm{Al}_i$*, according to Table 2*

Table 3

Flexural properties of tested specimens

	E_f, MPa	$\sigma_{0.2f}$, MPa	$\sigma_{\max f}$, MPa	$\varepsilon_{\max f}$, %
Alu	5,452	52	90	4
C1	32,611	119	166	2.8
C2	32,940	129	187	3.4
C3	42,477	147	246	6.3

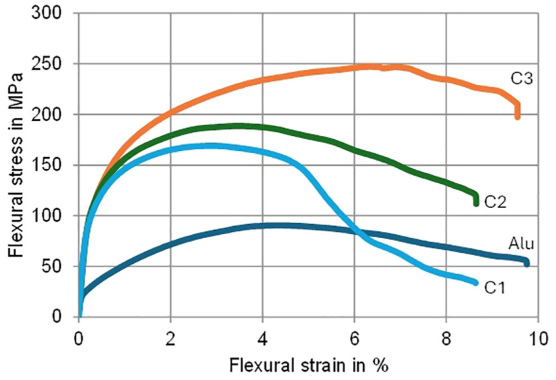

a

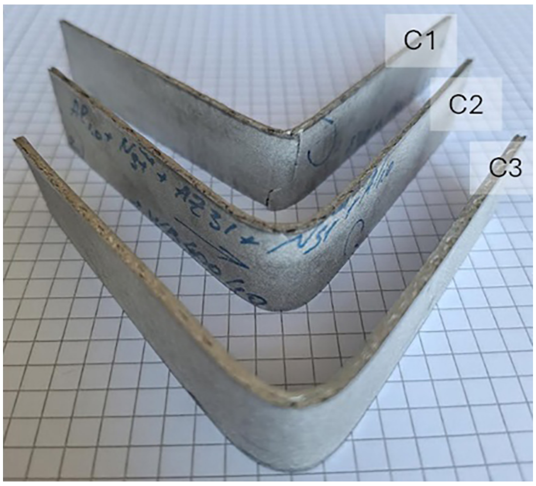

b

Fig. 5. The three-point bending test results in flexural stress-strain curves (a) and changes to the visual appearance of composites C1, C2 and C3 (b)

C2 exhibited an average strength value within the series, as well as moderate ductility.

C3 demonstrated the best properties, showing high strength and resistance to deformation without damage. Its bent shape (Fig. 5, *b*) is the most uniform, confirming the combination of stiffness and ductility in this composite. The residual bending angle is less than 90°.

Ball indentation tests. Fig. 6 shows graphs of the load versus ball displacement and a photo of the specimen after the test, respectively.

The test results indicate that EN AW 1050 aluminium exhibits greater drawing capacity when the ball is pressed in, compared to the composites. However, the composites demonstrate greater stiffness. As in previous tests, this stiffness correlates with the state of the kirigami structure (Fig. 3).

The intact structure enables more energy to be absorbed during the initial moments of loading. This effect can be quantified by considering the amount of energy absorbed by the specimen. This energy can be calculated by determining the work of the load, which is represented by the area under the load-indentation curve. The mechanical work performed during deformation can be determined as follows

$$A = \int_0^l F(l) \cdot dl [J], \tag{5}$$

where $F(l)$ is the indentation force as a function of the indentation depth; dl is the load measurement step and dl is the indentation depth.

The unreinforced material will show better results if the performance is measured up to the point of sample fracture. This is due to the free movement of dislocations and other sources of ductility throughout the specimen's thickness. To evaluate the composite material's ability to absorb energy during the initial loading period, it is necessary to set a limit on the indenter ball's movement distance.

The choice of this distance for calculating the absorbed energy may be related to operating conditions or other factors. In the current study, 4 mm distance was chosen based on the absence of fractures in the specimens.

For a correct comparison of the energy absorbed by samples of different thicknesses, the specific value will be used

$$A'_{b4} = \frac{A_4}{h_i}, \tag{6}$$

where A_4 is the energy value at a distance of 4 mm of the ball indentation and h_i is the specimen thickness.

The values of the specific absorbed energy at the point of the first 4 mm of the ball's indentation A'_{b4} for the tested specimens were as follows: EN AW 1050 – $A'_{b4} = 1.29$ J/mm; C1 – $A'_{b4} = 1.69$ J/mm; C2 – $A'_{b4} = 1.92$ J/mm; C3 – $A'_{b4} = 2.25$ J/*mm*.

Therefore, despite the ductility advantages of the unreinforced material, the composite material produced by roll bonding exhibits a 74 % increase in energy absorption capacity in a complex stress-strain state.

The C3 composite demonstrated the most outstanding characteristics, as indicated by the test outcomes. This was attributed to the preservation of the kirigami

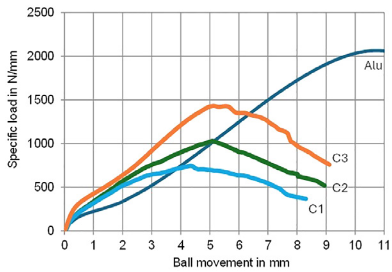

a

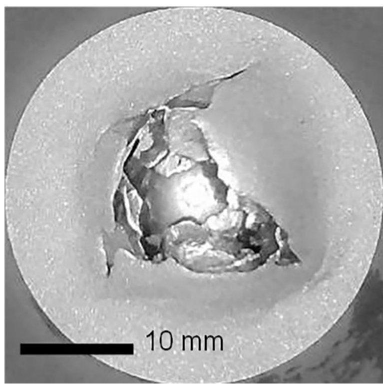

b

Fig. 6. Specific load diagram (a) and post-test view (b) obtained during the ball indentation test

structure integrity, which is formed through roll bonding with a 51 % reduction and an augmented mesh angle of 86° (whereas the initial angle α_y (refer to Fig. 2) was 62°). Its maximum impact resistance was 2.73 J/mm, which is 66 % higher than EN AW 1050 aluminium and 27 % higher than C2. In the three-point bending test, the C3 specimen reached a maximum stress of 246 MPa and a strain of 6.3 %, while the aluminium specimen reached only 90 MPa and 4 %, respectively. The tangent modulus of elasticity E_f of C3 was 42,477 MPa, which is 7.8 times higher than that of aluminium.

In the ball indentation test, the C3 composite demonstrated the highest energy absorption capacity, which was 74 % higher than that of EN AW 1050. Therefore, C3 composite combines high stiffness, strength and energy absorption capacity while maintaining the integrity of the kirigami structure.

The integrity of the kirigami structure is one of the key factors in determining the mechanical properties of roll-bonded composites. This integrity is determined by the longitudinal angle of the mesh after deformation. As can be seen in Fig. 3, increasing the longitudinal angle of specimens C1 and C2 from 62° to 118 and 114°, respectively, leads to cell fracture. The kirigami structure remains intact when the longitudinal mesh angle is set at 86° in sample C3.

Ensuring the isotropy of the composite properties requires the longitudinal mesh angle to be close to 90°, as demonstrated in previous studies [14].

All the composites considered in this study were rolled at a shape factor of between 2.9 and 4.0, i.e., the ratio of the length of the deformation zone to the average sheet thickness. Such values of the shape factor refer to the case of rolling thin bars, which minimises the deformation unevenness along the height of the composite and contributes to reliable connection of the layers inside. As demonstrated in [24], values of the shape factor in this range coincide with the zone of intensive growth of the mesh angle, a phenomenon that is amplified by the displacement of the kirigami structure from the rolling plane. Therefore, controlling the mesh deformation in such conditions is of great importance.

Mechanical tests, including impact bending, three-point bending and ball indentation, confirmed the high mechanical properties of the C3 composite, with no kirigami structure destruction observed. Such composites demonstrated a greater ability to absorb energy. Table 4 presents the generalised results of the effect of rolling reduction on the mechanical properties of composites obtained in the process of roll bonding five-layer composites consisting of aluminium and magnesium sheets with steel kirigami inlays.

According to Table 4, the change in the longitudinal mesh angle α_y in composites C1, C2 and C3 was 0.83, 0.84 and 0.5°, respectively, for each percentage of deformation, considering an initial angle of 62°. These results are in good agreement with those obtained for three-layer composites in [14, 15, 19].

Interpolation of the data in Table 4 indicates that, for the roll bonding conditions of the five-layer aluminium and magnesium alloy composites presented in this study, an outer mesh angle of 90° can be achieved with a rolling reduction of 55 %.

Table 4

A comparison of the deformation parameters and mechanical properties of composites with those of pure aluminium

Experiment code	α_y, °	ε, %	A'_{Imp}, $\frac{J}{mm}$	ε_{maxf}, %	σ_{maxf}, MPa	A'_{b4}, $\frac{J}{mm}$
Alu	–	–	1.64	4.0	90	1.29
C1	118	70	1.62	2.8	166	1.69
C2	114	64	2.08	3.4	187	1.92
C3	86	51	2.73	6.3	246	2.25

A comparison of the energy absorbed by the sample during impact tests and during ball indentation has shown that the composites are more resistant to the complex stress-strain state that occurs during ball indentation tests. The decrease in absorbed energy is 17.6 % for composite C3, 7.7 % for composite C2 and 21.4 % for aluminium. A 55 % rolling reduction results in a 14.6 % decrease in that index, highlighting the importance of isotropic properties in composites. These properties enable the composite to withstand complex stress conditions. Additionally, delamination during ball indentation provides a longer time window before through holes appear (Fig. 6).

Conclusions.

1. The mechanical properties of five-layer composites, consisting of two aluminium outer matrices, an inner magnesium matrix, and two steel kirigami inlays, depend on the initial configuration of these components and the rolling reduction during roll bonding.

2. These composites demonstrate a ball indentation energy of 2.25 J/mm with a 10 % increase in specific weight, which is 74 % higher than the 1.29 J/mm of unreinforced aluminium EN AW 1050. This is due to the controlled deformation of the kirigami structure during rolling with a 51 % reduction. Restricting the increase in the longitudinal mesh angle to 86° prevented cell destruction and maximised impact resistance to 2.73 J, 66 % higher than the base material. In three-point bending tests, a maximum stress of 246 MPa was achieved – 2.7 times higher than aluminium – demonstrating the high efficiency of the geometrically stable kirigami structure.

3. In order to preserve the integrity of the kirigami structure during rolling, it is necessary to ensure geometric balance between its elements. This prevents the local destruction of both the structure and the internal matrix. The proposed correlation between mesh parameters enables the rational design of cutout shapes, ensuring integral interaction between the structure and matrix under conditions of complex deformation.

4. The mechanical properties of composites depend on the state of the kirigami structure within the composite following roll bonding. This, in turn, depends on the value of the longitudinal angle of the mesh after rolling. In this study, a longitudinal angle of 114° was critical.

5. For the rolling-bonding of five-layer aluminium-magnesium composites, a rolling reduction value of 55 % is recommended to ensure reliable bonding of the layers and the achievement of isotropic properties. This

level of deformation also increases the composites' resistance to complex stress-strain conditions.

Acknowledgements. *The research was carried out as part of project No. 2023.04/0156, 'Development of technology for using kirigami-inspired structures in the thermal-deformation treatment of composite material sheets', funded by the National Research Foundation of Ukraine. The authors would like to thank Mikhail Rodman for sharing his magnesium rolling experience.*

References.

1. Simões, S. (2024). High-Performance Advanced Composites in Multifunctional Material Design: State of the Art, Challenges, and Future Directions. *Materials*, *17*, 5997. https://doi.org/10.3390/ma17235997

2. Bai, J., Yang, Y., Wen, C., Chen, J., Zhou, G., Jiang, B., Peng, X., & Pan, F. (2023). Applications of magnesium alloys for aerospace: A review. *Journal of Magnesium and Alloys*, *11*(10), 3609-3619. https://doi.org/10.1016/j.jma.2023.09.015

3. Hou, J., Li, D., Liu, Z., Ji, Z., Guan, S., Li, C., Qiao, X., Golovin, I., & Zheng, M. (2023). Structure-function integrated magnesium alloys and their composites. *Journal of Magnesium and Alloys*, *11*(10), 3511-3544. https://doi.org/10.1016/j.jma.2023.09.012

4. Wu, T., & Zhang, K. (2023). Corrosion and Protection of Magnesium Alloys: Recent Advances and Future Perspectives. *Coatings*, *13*(9), 1533. https://doi.org/10.3390/coatings13091533

5. Li, Z., Rezaei, S., Wang, T., Han, J., Shu, X., Pater, Z., & Huang, Q. (2022). Recent advances and trends in roll bonding c bonding model: A review. *Chinese Journal of Aeronautics*, *36*(4), 36-74. https://doi.org/10.1016/j.cja.2022.07.004

6. Szabó, G. (2017). Optimization of Roll Bonding by Hot Rolling in Experimental and Industrial Use. *Archives of Metallurgy and Materials*, *62*, 1205-1208. https://doi.org/10.1515/AMM-2017-0178

7. Saleh, H., Schmidtchen, M., & Kawalla, R. (2018). Hot Roll Bonding of Aluminum to Twin-Roll Cast (TRC) Magnesium and Its Subsequent Deformation Behavior. *Journal of Materials Engineering and Performance*, *27*, 5069-5078. https://doi.org/10.1007/s11665-018-3217-x

8. Abbasi, M., & Sajjadi, S. (2018). Mechanical Properties and Interface Evaluation of Al/AZ31 Multilayer Composites Produced by ARB at Different Rolling Temperatures. *Journal of Materials Engineering and Performance*, *27*, 3508-3520. https://doi.org/10.1007/s11665-018-3423-6

9. Tiamiyu, A., Chen, X., Pangv, E., Sun, Y., Lienhard, J., Lebeau, J., Nelson, K., & Schuh, C. (2021). Oxide layer delamination: an energy dissipation mechanism during high-velocity microparticle impacts. *Applied Surface Science*, *574*, 151673. https://doi.org/10.1016/j.apsusc.2021.151673

10. Lienhard, J., Crook, C., Azar, M., Hassani, M., Mumm, D., Veysset, D., ..., & Valdevit, L. (2020). Surface oxide and hydroxide effects on aluminum microparticle impact bonding. *Acta Materialia*, *197*, 28-39. https://doi.org/10.1016/j.actamat.2020.07.011

11. Zhang, X., Luo, Z., Xie, G., Yu, H., Liu, Z., & Yang, J. (2022). Interface microstructure and bonding mechanisms of 7050 aluminum alloy thick plates produced by vacuum roll cladding. *Materials Science and Engineering: A*, *850*, 143582. https://doi.org/10.1016/j.msea.2022.143582

12. Yang, Y., Jiang, Z., Chen, Y., Liu, X., Sun, J., & Wang, W. (2022). Interfacial microstructure and strengthening mechanism of stainless steel/carbon steel laminated composite fabricated by liquid-solid bonding and hot rolling. *Materials Characterization*, *191*, 112122. https://doi.org/10.1016/j.matchar.2022.112122

13. Demler, E., Rodman, D., Rodman, M., Gerstein, G., Grydin O., Briukhanov, A., ..., & Maier, H. Y. (2018). The influence of alternating low-cycle bending loads on sheet properties having an HCP crystal lattice. *Journal of Materials Engineering and Performance, 27*(2), 541-549. https://doi.org/10.1007/s11665-018-3123-2

14. Frolov, Y., Haranich, Y., Bobukh, O., Remez, O., Voswinkel, D., & Grydin, O. (2020). Deformation of expanded steel mesh inlay inside aluminum matrix during the roll bonding. *Journal of Manufacturing Processes, 58*, 857-867. https://doi.org/10.1016/j.jmapro.2020.08.049

15. Frolov, Y., Nosko, M., Samsonenko, A., Bobukh, O., & Remez, O. (2021). Roll Bonding of Al-Based Composite Reinforced with C10 Steel Expanded Mesh Inlay. *Metals*, *11*, 1044. https://doi.org/10.3390/met11071044

16. Liu, T., Song, B., Huang, G., Jiang, X., Guo, S., Zheng, K., & Pan, F. (2022). Preparation, structure and properties of Mg/Al laminated metal composites fabricated by roll-bonding, a review. *Journal of Magnesium and Alloys*, *10*(8), 2062-2093. https://doi.org/10.1016/j.jma.2022.08.001

17. Tao, J., Khosravi, H., Deshpande, V., & Li, S. (2022). Engineering by Cuts: How Kirigami Principle Enables Unique Mechanical Properties and Functionalities. *Advanced Science*, *10*, 2204733. https://doi.org/10.1002/advs.202204733

18. Jin, L., Forte, A. E., Deng, B., Rafsanjani, A., & Bertoldi, K. (2020). Kirigami-Inspired Inflatables with Programmable Shapes. *Advanced Materials*, *32*(33), 2001863. https://doi.org/10.1002/adma.202001863

19. Frolov, Y., Konovodov, D., Bobukh, O., & Boiarkin, V. (2025). Transformation of the kirigami-type deformable inlay during roll bonding. *Naukovyi Visnyk Natsionalnoho Hirnychoho Universytetu*, (1), 34-39. https://doi.org/10.33271/nvngu/2025-1/034

20. Raisie, F., Sedighi, M., & Rouzbeh, A. (2023). An Experimental Study on the Creep Behavior of Al 1050/Mg AZ31B Bilayer Sheet Fabricated via Roll Bonding. *Journal of Materials Engineering and Performance*, *33*, 12467-12479. https://doi.org/10.1007/s11665-023-08819-z

21. Taniyama, H., & Iwase, E. (2021). Design of a Kirigami Structure with a Large Uniform Deformation Region. *Micromachines*, *12*, 76. https://doi.org/10.3390/mi12010076

22. Soleimani, H., Goudarzi, T., & Aghdam, M. (2021). Advanced structural modeling of a fold in Origami/Kirigami inspired structures. *Thin-walled Structures*, *161*, 107406. https://doi.org/10.1016/J.TWS.2020.107406

23. Rashidi, M., Tayebi, P., & Hashemi, R. (2025). Stress relief treatment of aluminum/magnesium laminates fabricated by roll bonding technique. *Heliyon*, *11*(2), e41639. https://doi.org/10.1016/j.heliyon.2025.e41639

24. Frolov, Y., Bobukh, O., Samsonenko, A., & Nurnberger, F. (2023). Patterning of Surfaces for Subsequent Roll Bonding in a Low-Oxygen Environment Using Deformable Mesh Inlays. *Journal of Manufacturing Processes*, *7*(5), 158. https://doi.org/10.3390/jmmp7050158

25. Liu, Z., Krämer, A., Lohmar, J., Aretz, H., Karhausen, K., Bailly, D., Hirt, G., & Teller, M. (2023) The adaption, evaluation and application of a semi-empirical bond strength model for the simulations of multi-pass hot roll bonding of aluminium alloys. *International Journal of Material Forming, 16*, 71. https://doi.org/10.1007/s12289-023-01795-8

Вплив параметрів деформування при прокатці-з'єднанні на механічні властивості алюмінієво-магнієвих композитів із кірігамі-вставками

Я. В. Фролов[1], *Ф. Нюрнбергер*[2], *Д. В. Коноводов*[*1], *О. С. Бобух*[1], *В. В. Бояркін*[1]

1 – Український державний університет науки і технологій, м. Дніпро, Україна

2 – Ляйбниц Університет, м. Ганновер, Федеративна Республіка Німеччина

[*] Автор-кореспондент e-mail: d.v.konovodov@ust.edu.ua

Мета. Оцінка залежності механічних властивостей композиційного матеріалу, що складається з алюмінію EN AW 1050, структури кірігамі зі сталі E235 і магнієвого сплаву AZ31, від початкової конфігурації його складових і обтиску при прокатці-з'єднанні.

Методика. Дослідження включало отримання методом прокатки-з'єднання п'ятишарових композитних листів такої конфігурації: два внутрішні шари складалися з кірігамі-структури, у якості якої використовували просічно-витяжну сітку з низьковуглецевої сталі; у якості зовнішніх матричних шарів використовували листи з алюмінієвого сплаву, а внутрішнього матричного шару – лист зі сплаву магнію. Стан кірігамі-структури оцінювали за допомогою рентгенівського аналізу. Механічні властивості отриманих композитів оцінювали трьома методами: випробування на ударний вигин; триточковий вигин; випробування на вдавлювання кульки.

Результати. За результатами експериментального дослідження були отримані дані про трансформацію кірігамі-структури в середині п'ятишарового композиту в залежності від величини відносного обтиску. Встановлено, що забезпечення ізотропії властивостей композиту можливо за умови дотримання деформації при прокатці на рівні 55 %. Результати механічних випробувань показали, що армування кірігамі-структурою на 60–70 % підвищує здатність до поглинання енергії, у тому числі в умовах складного напружено-деформованого стану. Жорсткість таких композитів у декілька разів вища за жорсткість неармованого алюмінію.

Наукова новизна. У даному дослідженні вперше кількісно оцінено вплив конфігурації компонентів і відносного обтиску при прокатці на механічні властивості п'ятишарового алюмінієво-магнієвого композиту, армованого сталевою кірігамі-структурою. Встановлено, що параметри деформації забезпечують не тільки надійне з'єднання шарів магнію й алюмінію, а ще, за рахунок контрольованої трансформації кірігамі-структури, значне збільшення показників механічних властивостей.

Практична значимість. Результати дослідження розширюють уявлення про вплив обтиску й початкової конфігурації шарів багатошарового алюмінієво-магнієвого композиту на його деформацію під час прокатки-з'єднанні та можуть бути основою для розробки нових композитів, армованих кірігамі-структурами.

Ключові слова: *прокатка-з'єднання, кірігамі-структура, композитний матеріал, питома міцність*

The manuscript was submitted 07.04.25.